ANALYSIS AND DESIGN OF A HYPERSONIC SCRAMJET ENGINE WITH A TRANSITION MACH NUMBER OF 4.79

Article · SEPTEMBER 2021

DOI: 10.251IRS104758ISCA

2 authors, including:

DR.DIPESH SATPATI{SPACE REASEARCHER,IRS104758ISCA}

INDIAN SPACE RESEARCH ORGANISATION

25PUBLICATIONS **3000** CITATIONS

POST DOCTORAL RESEARCHER

SEE PROFILE

AIAA 2021-104758

Analysis and Design of a Hypersonic Scramjet Engine with a Transition Mach Number of 4.79

DR. DIPESH SATPATI[1] and DR. PRASANTA BANERJEE[2]
INDIAN SPACE RESEARCH ORGANISATION ISRO26021

When pressures and temperatures become so high in supersonic flight that it is no longer efficient to slow the oncoming flow to subsonic speeds for combustion, a scramjet (supersonic combustion ramjet) is used in place of a ramjet. Currently, the transition to supersonic combustion generally occurs at a freestream Mach number around 5.0 to 6.0. This research details analysis completed towards extending scramjet operability to lower Mach numbers, while maintaining performance at higher Mach numbers within the same flowpath as detailed in the Air Force solicitation AF073-058. The specific goal was to determine whether the scramjet starting Mach number could be lowered to Mach 3.50 and, if not, what the constraints are that prohibit it and what the lowest possible starting Mach number for a scramjet is with today's technology. This analysis has produced many significant insights into the current and required capabilities for both fuel and overall engine design in lowering the starting Mach number; these results are presented here. The analysis has shown that a scramjet with a starting Mach number of 3.50 is not currently possible with the fuels researched unless fuel additives or other modifications to the system are used. However, a scramjet with a starting Mach number of 4.00 is possible with today's existing technology. This paper has designed the engine flowpath for this case; its specifications and resulting performance are also detailed here.

Nomenclature

M_i	*Mach Number at Station i*
T_3/T_0	*Ratio of Burner Entry Temperature to Freestream Temperature*
φ	*Ratio of Burner Entry Temperature to Freestream Temperature*
γ	*Ratio of Specific Heats*
f	*Fuel-to-Air Ratio*
f_{st}	*Stoichiometric Fuel-to-Air Ratio*
PDE	*Pulsed Detonation Engine*
T_{t0}	*Stagnation Temperature of Freestream Air*
Cp	*Specific Heat*
V_i	*Axial Velocity at Station i*
p_i	*Static Pressure at Station i*
S	*Specific Fuel Consumption*
T_i	*Static Temperature at Station i*
n_o	*Overall Efficiency*
n_{th}	*Thermal Efficiency*
n_p	*Propulsive Efficiency*
n_c	*Inlet Compression System Efficiency*
n_b	*Burner Efficiency*
n_e	*Expansion System Efficiency*
n_{KE}	*Kinetic Energy Efficiency*
I_{sp}	*Specific Impulse*
$F \mid \dot{m}_0$	*Specific Thrust*
x	*Axial Location*
xi	*Axial Location of Fuel Injection*

[1] Space Scientist, Indian Space Research Organisation,ISRO BANGALORE, Post Doctoral Researcher,isc Ahmedabad.,
[2] Professor, Mechanical and Aerospace Engineering, Indian Space Research Organisation,ISRO BANGALORE, Associate Fellow, AIAA.

y	*Distance Perpendicular from the Axial Direction*
h	*Distance Perpendicular from the Axial Direction, Equivalent to y*
z	*Distance Perpendicular from the x-y Plane*
d	*Distance Perpendicular from the x-y Plane, Equivalent to z*
R	*Perfect Gas Constant*
R_b	*Perfect Gas Constant in Burner*
h_{PR}	*Heat Of Reaction*
T_i/T_0	*Ratio of Static Temperature at Station i to Freestream Static Temperature*
p_i/p_0	*Ratio of Static Pressure at Station i to Freestream Static Pressure*
A_i/A_0	*Ratio of Area at Station i to Inlet Area*
P_{ti}/P_{t0}	*Ratio of Total Pressure at Station i to Freestream Total Temperature*
$(s_i-s_0)/C_p$	*Dimensionless Entropy Increase Between Station i and the Inlet*
θ/H	*Ratio of Boundary Layer Momentum Thickness to Duct Height*
H	*Height*
θ	*Empirical Constant Based on Mode of Fuel Injection and Fuel-Air Mixing*
μ_i	*Mach angle at a Mach number of i*
IT	*Ignition Temperature*
πc	*Total Pressure Ratio*
Φ	*Stream Thrust Function*
T^o	*Reference Temperature*
K	*Dimensionless Kinetic Energy*
H	*Dimensionless Static Enthalpy*
Sa_i	*Stream Thrust Function at Station i*
$SERN$	*Single Expansion Ramp Nozzle*
ϕ	*Equivalence Ratio*

I. Introduction

Figure 1 below is a good summary of the current challenges in the development of the scramjet engine. There are four major areas that these problems lay in, namely Air Induction, Combustor, Nozzle, and Structures and Materials. Problems within these areas vary from inlet starting problems to the inherent difficulty of igniting the fuel in a supersonic flow, as the possibility of failure exists anywhere from the fuel not igniting to the ignition taking place outside of the combustor due to the extraordinary velocity of the air in the engine. Additionally, structures that can withstand the extreme temperatures experienced during hypersonic flight combined with the additional temperatures experienced during combustion are necessary.

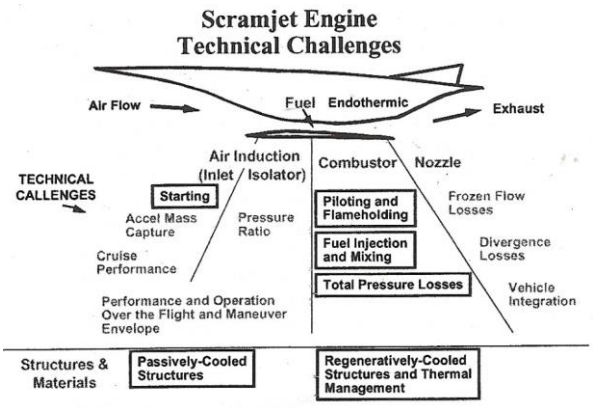

Figure 1: Technical Challenges of Scramjet Engine Development [1]

In addition to these technical challenges, there is another area of scramjet development which deserves attention. Despite the wide range of applications possible with scramjet technology, the vehicle must first be propelled to a high enough Mach number for the scramjet to start. This requires, depending on the intended application, one or two additional propulsion systems to propel the vehicle to the required scramjet start velocity. Current scramjet designs target the start of supersonic combustion to be between Mach 5 and 6 [2, 3, 4]. In order to minimize the weight and complexity of having multiple propulsion systems, a dual-mode ramjet/scramjet is often proposed. However, if the

necessary scramjet starting Mach number is reduced, a reduction in the number of required additional propulsion systems is possible, as the gap is bridged between the maximum possible velocity of the low speed engine(s) and the scramjet start velocity. This would have direct advantages from the resulting reduction in overall vehicle weight, the lower mass fraction required for the propulsion system (thereby resulting in more available payload weight), and fewer systems that must work in succession reliably, thereby increasing overall vehicle safety. The focus of this project is to address this issue of reducing the starting Mach number.

Air Force Solicitation AF073-058 stated that a critical path issue in scramjet development is for scramjet operability to be extended to lower Mach numbers. Specifically, the solicitation stated that scramjet start should be reduced to "Mach 3.50 while maintaining performance at higher Mach numbers within the same flowpath" with minimal variable geometry features and the use of hydrocarbon fuel [5]. According to Fry [3], a turbojet engine can provide for thrust from takeoff to a speed of Mach 3 or 4. Therefore, if a scramjet were designed with a starting Mach number of about 3.50, presumably only two propulsion systems would be needed for the entire mission, whether that is up to Mach 8-10 for a hydrocarbon-powered scramjet [2] or up to Mach 15-20 for a hydrogen-powered scramjet [2]. The advantage of this approach is clear due to the reasons discussed above—overall weight reduction, higher payload capacity, and increased vehicle reliability and safety. The motivation for the problem, therefore, is to enable takeoff to hypersonic flight to be achieved using only a turbojet and a scramjet, with no ramjet cycle in between.

There are a few key parameters of the "pure" scramjet engine—that is, a scramjet with one combustor and a non-variable flowpath—that are able to be varied and manipulated to perhaps lower the starting Mach number of a scramjet. For instance, as the cycle static temperature ratio (T_3/T_0) increases, the Mach number of the flow entering the burner (M_3) decreases [2]. Thus, T_3/T_0 directly affects the freestream Mach number (M_0) at which the flow entering the burner (M_3) becomes supersonic. Due to this, it is possible that the manipulation of T_3/T_0 would yield a lower freestream Mach number at which supersonic combustion can occur. Additionally, the key design parameters of fuel selection and fuel-to-air ratio (*f*) for the scramjet may have an impact on the starting scramjet Mach number. The manipulation of these pure scramjet key design parameters is the approach used in the current project.

II. Analysis of Key Design Parameters to Reduce Scramjet Starting Mach Number

The reference station designations used in this analysis are those used by Heiser and Pratt [2] and can be seen below in Figure 2.

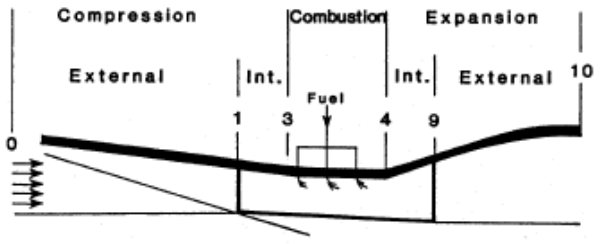

Reference Station	Engine Location
0	Undisturbed or freestream conditions
	External compression begins
1	External compression ends
	Internal compression begins
	Inlet or diffuser entry
3	Inlet or diffuser exit
	Internal compression ends
	Burner or combustor entry
4	Burner or combustor exit
	Internal expansion begins
	Nozzle entry
9	Internal expansion ends
	Nozzle exit
	External expansion begins
10	External expansion ends

Figure 2: Scramjet Reference Station Designations [2]

Table 1 lists the one-dimensional stream thrust performance analysis inputs and how they are determined. As seen in the table, the vast majority of the inputs are set by the freestream Mach number, are properties that remain constant for air, earth, etc., or are assumed based on reasonable values within a typical range. The values for the constant and assumed inputs can be seen in Table 2 below. These values are used throughout the project for all analysis calculations as needed unless otherwise noted. All assumed values were chosen based on recommendations from Reference 2. Additionally, all constants were determined based on information in Reference 2.

Table 1: Performance Analysis Inputs and Corresponding Determination Methods

Performance Analysis Inputs	How Determined
M_0, V_0, T_0, p_0	Set by Mach Number
C_{pc}, R, C_{pb}, C_{pe}, h_f, g_o	Constant
V_{fx}/V_3, V_f/V_3, $C_f(A_w/A_3)$, n_c, n_b, n_e, T_0, p_{10}/p_0, γ_c, γ_e, γ_b	Assumed
T_3/T_0, f, h_{pr}	Variation

Table 2: Stream Thrust Inputs: Values for Constant and Assumed Values

Constants [1]		
C_{pc}	1090.00	J/kgK
R	289.3	$(m/s)^2/K$
C_{pb}	1510.00	J/kgK
C_{pe}	1510.00	J/kgK
h_f	0.00	
g_0	9.81	m/s^2
Assumed Values [1]		
V_{fx}/V_3	0.50	
V_f/V_3	0.50	
$C_f{}^*A_w/A_3$	0.10	
η_c	0.90	
η_b	0.90	
η_e	0.90	
T^0	222.00	K
p_{10}/p_0	1.40	
γ_c	1.362	
γ_e	1.238	
γ_b	1.238	

In order to accurately assess whether a scramjet starting Mach number of 3.50 is possible or worthwhile, performance analysis was completed to determine whether the necessary T_3/T_0 is achievable. Additionally, performance analysis was performed to parametrically vary the engine parameters of fuel-to-air ratio and fuel properties to determine whether a scramjet with a starting Mach number of 3.50 is possible.

In this analysis, a one-dimensional flow approach was used. As Heiser and Pratt explain, "although the one-dimensional approach can never be perfectly correct, the alternatives are both hopelessly complex and completely unwieldy for reaching a basic understanding built upon fundamental principles" [2]. For the current project, a complex analysis was not needed. The one-dimensional flow approach assumes that the fluid properties remain constant across the flow and thus only depend on the axial dimension coordinate [2]. This serves as an excellent method for the current project, as the flow within a scramjet engine is confined within the definite boundaries of the engine flowpath, making a two- or three-dimensional analysis unnecessary for achieving an understanding of the flow [2].

The Stream Thrust Analysis method has been employed here, as it accounts for the most engine parameters and influences compared to other one-dimensional flow analysis methods. This method requires more initial information than other one-dimensional methods and uses the entire set of control volume conservation equations [2]. It leans heavily on momentum relationships and offers a different approach than the one-dimensional energy methods [2].

A. Theory and Equations

This section briefly lists the equations used in the analysis. For more detailed equations and explanations, please see Reference 6.

The largest factor in changing the freestream Mach number at which supersonic combustion begins is the cycle static temperature ratio, T_3/T_0. As T_3/T_0 increases for a given freestream Mach number (M_0), the Mach number of the flow entering the combustor decreases [2]. Thus, T_3/T_0 directly affects the M_0 at which the flow entering the burner (M_3) becomes supersonic. So, with a range of freestream Mach numbers, the necessary T_3/T_0 can be determined based on M_0 and the ratio of specific heats at compression (γ_c) where M_3=1 by the following equation [2]:

$$M_3 = \sqrt{\frac{2}{\gamma_c - 1}\left[\frac{T_o}{T_3}\left(1 + \frac{\gamma_c - 1}{2} M_o^2\right) - 1\right]} \tag{1}$$

This preliminary calculation serves an adequate way to get an estimate of the required T_3/T_0 value to lower the starting Mach number of the scramjet.

For the full theoretical analysis, the control volume is defined as in Figure 3. In this definition, the outside surface of the engine lines up with the dividing streamlines that constitute the internal and external flow boundaries [2].

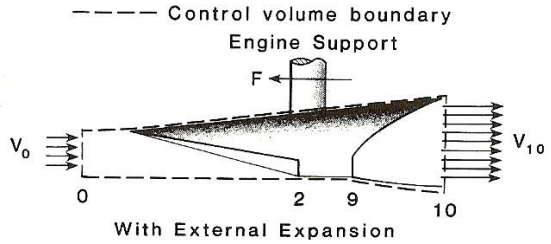

Figure 3: Scramjet Control Volume Definition [2]

This one-dimensional flow analysis method assumes that all of the flow through the engine is aligned in the axial direction, and therefore, that the throughflow area is perpendicular to the axial [2]. Also, it is assumed that the perfect gas constant (R) is constant across the engine, as the molecular weight of air does not vary enough across the engine to make a significant difference in the calculations [2]. Heiser and Pratt note that the perfect gas law was used "repeatedly to eliminate density from the equations" and that p_{10}/p_0 is treated as an independent parameter in the equations for this analysis [2].

It is best to break the engine down into separate functional parts, as "significantly different physical phenomena are at work in each"; therefore, this analysis operates with the following component breakdown [2]:

1. ***Compression Component (Reference Stations 0 to 3):*** Includes compression surfaces (internal and external), isolator, intake, etc. up to the combustor entrance.
2. ***Combustion Component (Reference Stations 3 to 4):*** Consists of the combustor and all parts that make combustion happen including fuel injectors, etc. that lie within the combustor.
3. ***Expansion Component (Reference Stations 4 to 10):*** Includes all expansion surfaces after the combustor exit up to the engine exit.

With the component breakdown established, it is now possible to step through the equation set of this analysis method. Please observe the symbolic definitions and abbreviations located at the beginning of this paper. All equations listed below are taken directly from Reference 2.

<u>Compression Component (Reference Stations 0 to 3)</u>

1. Stream thrust function at freestream conditions

$$Sa_0 = V_0\left(1 + \frac{RT_0}{V_0^2}\right) \tag{2}$$

2. Combustor entrance temperature

$$T_3 = \varphi T_0 \tag{3}$$

3. Combustor entrance velocity

$$V_3 = \sqrt{V_0^2 - 2C_{pc}T_0(\varphi - 1)} \tag{4}$$

4. Stream thrust function at combustor entrance

$$Sa_3 = V_3\left(1+\frac{RT_3}{V_3^2}\right) \tag{5}$$

5. Ratio of combustor entrance pressure to freestream pressure

$$\frac{p_3}{p_0} = \frac{\varphi}{\varphi(1-\eta_c)+\eta_c}\left(\frac{C_{pc}}{R}\right) \tag{6}$$

6. Ratio of combustor entrance area to freestream entrance area

$$\frac{A_3}{A_0} = \varphi \cdot \frac{p_0}{p_3} \cdot \frac{V_0}{V_3} \tag{7}$$

<u>Combustion Component (Reference Stations 3 to 4)</u>

There are two methods for calculating the combustion properties, depending on the type of combustor designed: constant-pressure or constant-area combustion. The constant-pressure combustor is able to achieve results closest to ideal, since it is designed to conserve pressure, therefore generating less total pressure loss which in turn gives the engine a higher overall efficiency. Therefore, this is the combustor that has been used in the current project and the combustor type to which the proceeding equations apply.

However, there are some considerations to be made before these equations are listed. An absolutely constant-pressure burner is not feasible in terms of current manufacturing capabilities [2], so the application of an isolator which prevents inlet unstart is used. Additionally, the burner walls must be more or less straight with a small variation in area in the axial direction [2]. A constant ratio of the area at the combustor exit to entrance is instilled; that is, variable geometry will not be used. The combination of a small variation in axial area combined with the use of an isolator helps to achieve nearly equal pressures from the burner entry to the burner exit [2]. The following equations apply to the constant-pressure combustor case. Please note, as this is a constant-pressure burner design, $p_4/p_0=p_3/p_0$ is assumed.

1. Combustor exit velocity

$$V_4 = V_3\left(\frac{1+f\cdot\frac{V_{fx}}{V_3}}{1+f}\right)\sqrt{C_f\cdot\frac{A_w}{A}\cdot\frac{1}{2(1+f)}} \tag{8}$$

2. Combustor exit temperature

$$T_4 = \frac{T_3}{1+f}\left(1+\frac{1}{C_{pb}T_3}\left(\eta_b' f h_{PR} + f h_f + f C_{pb} T^o + (1+f)\left(\frac{V_3^2}{2} - \frac{V_4^2}{2}\right)\right)\right) \tag{9}$$

3. Ratio of area at combustor exit to combustor entrance

$$\frac{A_4}{A_3} = (1+f)\cdot\frac{T_4}{T_3}\cdot\frac{V_3}{V_4} \tag{10}$$

4. Stream thrust function at combustor exit conditions

$$Sa_4 = V_4\left(1+\frac{RT_4}{V_4^2}\right) \tag{11}$$

Expansion Component (Reference Stations 4 to 10)

1. Temperature at engine exit

$$T_{10} = T_4\left(1-\eta_e'\left(1-\frac{p_{10}}{p_4}\cdot\frac{p_4}{p_0}\right)^{R/C_{p_c}}\right) \tag{12}$$

2. Velocity at engine exit

$$V_{10} = \sqrt{V_4^2 + 2C_{p_c}(T_4 - T)_{10}} \tag{13}$$

3. Stream thrust function at engine exit conditions

$$Sa_{10} = V_{10}\left(1+\frac{RT_{10}}{V_{10}^2}\right) \tag{14}$$

4. Ratio of area at engine exit to area at freestream entrance

$$\frac{A_{10}}{A_0} = (1+f)\cdot\frac{p_0}{p_{10}}\cdot\frac{T_{10}}{T_0}\cdot\frac{V_0}{V_{10}} \tag{15}$$

Overall Engine Performance Measures (Across Stations 0 to 10)

With the analysis equations defined for the three engine components, it is now possible to establish the equations necessary to evaluate overall engine performance. These equations are shown below, and also taken directly from Reference 2.

1. Specific thrust

$$\frac{F}{\dot{m}_0} = (1+f)Sa_{10} - Sa_0 - \frac{R_0T_0}{V_0}\left(\frac{A_{10}}{A_0}-1\right) \tag{16}$$

2. Specific fuel consumption

$$S = \frac{f}{F/\dot{m}_0} \tag{17}$$

3. Specific impulse

$$I_{sp} = \frac{h_{PR}}{g_0 V_0}\eta_0 \tag{18}$$

4. Overall efficiency

$$\eta_0 = \frac{V_0}{h_{PR}S} \tag{19}$$

5. Thermal efficiency

$$\eta_{th} = \frac{\Upsilon \quad V^2/V^2}{\leq \quad 2 \quad f \quad 2} \qquad (20)$$

6. Propulsive efficiency

$$\eta_p = \frac{\eta_0}{\eta_{th}} \qquad (21)$$

7. Mach number

$$M = \frac{V}{\sqrt{\gamma RT}} \qquad (22)$$

A constant dynamic pressure (q) trajectory is applied and is used to determine the corresponding performance for a scramjet at a starting Mach number of 3.50 with a T_3/T_0 of 2.75 (this initial temperature ratio was determined by the analysis detailed in Section B below.) The trajectory was determined by using a constant q value of 47,880 N/m^2 in the Trajectory program of the Heiser and Pratt software "HAP" (Hypersonic Airbreathing Propulsion) [2]. This trajectory can be seen in Figure 4 below.

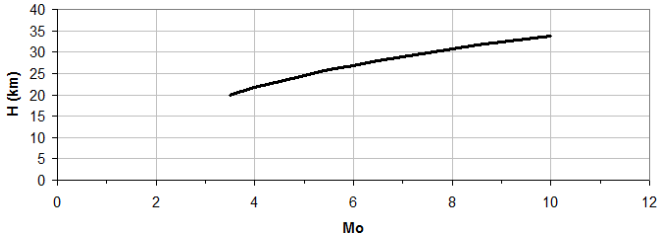

q_o	47880.26	N/m^2			
η_c	0.9				
γ_c	1.362				
M	Vo (m/s)	H (m)	H (km)	To (K)	po (Pa)
3.5	1032.74	19936.97	19.94	216.65	5582
4	1184.56	21646.90	21.65	218.22	4275
4.5	1337.23	23167.85	23.17	219.73	3377
5	1490.40	24539.45	24.54	221.09	2736
5.5	1644.02	25786.08	25.79	222.33	2260
6	1798.05	26929.08	26.93	223.47	1900
6.5	1952.46	27989.78	27.99	224.52	1619
7	2107.21	28974.29	28.97	225.49	1397
7.5	2262.29	29894.78	29.89	226.41	1217
8	2417.68	30760.42	30.76	227.26	1069
10	3061.05	33790.13	33.79	233.16	684

Figure 4: Constant Dynamic Pressure (q_0=47,880 N/m^2) Trajectory for Scramjet

B. Analysis: Variation of Cycle Static Temperature Ratio

The required value of T_3/T_0 to achieve a starting scramjet Mach number of 3.50 is determined using Equation 1. Using a range of freestream Mach numbers and γ_c=1.36 [2], the necessary T_3/T_0 for each freestream starting Mach number can be determined where $M_3 \geq 1$. The result can be seen in Figure 5.

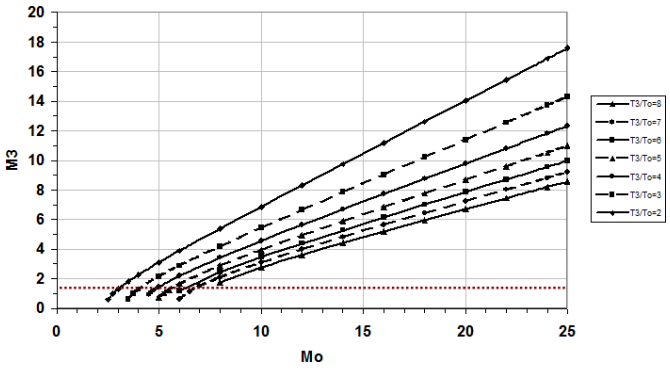

Figure 5: M_3 as a Function of M_0 and Cycle Static Temperature Ratio

As seen in Figure 5, the T_3/T_0 at which supersonic flow is achieved at the entrance to the combustor around Mach 3.5 is between 2 and 3. Specifically, solving Equation 1 with M_0=3.50, γ_c=1.36, and providing M_3 with a 10% margin by equating it to 1.10, gives a T_3/T_0 of 2.63. Figure 6 illustrates that for the target starting Mach number of 3.50, the required T_3/T_0 is approximately 2.75 solely based on M_0 and γ_c where $M_3 \geq 1$.

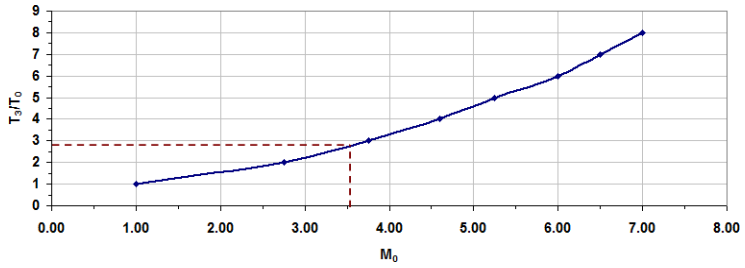

Figure 6: M_0 as a Function of Cycle Static Temperature Ratio

Therefore, preliminary calculations show that a T_3/T_0 approximately equal to 2.75 would allow for a scramjet starting Mach number of 3.50. However, the stream thrust analysis shows that for the constant-q trajectory, with M_0=3.50, T_3/T_0=2.75, a standard fuel-to-air ratio (*f*) of 0.04 [2], and a standard fuel heat of reaction (h_{PR}) of 87806.5 kJ/kg [2] (which falls between hydrogen and methane's heats of reaction), supersonic combustion is not maintained.

Repeating the analysis with the stipulation that supersonic combustion be maintained produces the results shown in Table 3 for various freestream Mach numbers.

Table 3: T_3/T_0 Required for Each Lowered Starting Mach Number

Mo	T3/To	M3	M4
3.5	1.25	2.98	1.00
3.75	1.50	2.78	1.01
4	1.75	2.64	1.02
4.25	2.00	2.54	1.04
4.5	2.50	2.22	1.00

The maximum T_3/T_0 possible for a generic scramjet with a starting Mach number of 3.50 to maintain supersonic combustion throughout the combustor is 1.25. However, this value of T_3/T_0 does not produce reasonable performance results and is therefore not a viable option. In light of this, fuel selection has been analyzed to determine if a higher value of T_3/T_0 is possible through the use of a different fuel to produce supersonic combustion as well as viable performance results.

C. Analysis: Fuel Selection

Many hydrogen and hydrocarbon fuels were researched as possible options for reducing the scramjet starting Mach number. Collected findings for advantages and disadvantages of each can be seen in Tables 4 and 5 below.

Table 4: Hydrogen Fuel Advantages and Disadvantages

	Advantage	Disadvantage
Hydrogen Fuel	Rapid burning [15]	Very low density [15, 17]
	High mass-specific energy content [15, 17]	Boil-off problems [15]
	Shortest ignition delay [9]	Requires largest vehicle size [8]

Table 5: Hydrocarbon Fuel Advantages and Disadvantages

	Advantage	Disadvantage
Hydrocarbon Fuels	Storable [15]	Slow burning [15]
	Handling is familiar [9, 15, 16]	Long ignition delay time [16]
	11 times the storage density of hydrogen [15]	Require quick vaporization before mixing [16]
	3.5 times more energy content per volume than hydrogen [15]	Exposing to high temperatures can result in coking [9, 17]
	Some offer smaller vehicles, logistic simplicity [8]	
	Safer to handle than hydrogen [9]	
	Realistic ground testing in existing facilities is possible [9]	

This research selected seven fuels which represented the widest spectrum of possible fuels and also held promise for the project at hand. The fuels selected and their corresponding heats of reaction can be seen below in Table 6 in descending order.

Table 6: Heats of Reaction of Fuels for Analysis [2, 7, 8]

Fuel Type	hPR (kJ/kg Fuel)
Hydrogen	119954.00
Methane	50010.00
Ethane	47484.00
Hexane	45100.00
Octane	44786.00
JP-7	43903.25
JP-10	42100.00

Additionally, each fuel's corresponding ignition temperature is listed in Table 7 in descending order. This is important, as the ignition temperature (IT) of a fuel is the temperature at which the fuel will self-ignite in air without a flame source or spark. The IT of the various fuels is very important for the current project, as a scramjet with a starting Mach number of 3.50 will have relatively low air temperatures, therefore requiring the fuel to be able to ignite at those temperatures [1].

Table 7: Ignition Temperatures of Fuels for Analysis at 1 atm [9, 10, 11]

Fuel Type	IT (K)
Hydrogen	845.15
Methane	810.15
Ethane	745.15
JP-10	518.15
JP-7	514.15
Hexane	498.15
Octane	479.15

The stoichiometric fuel-to-air ratio (f_{st}) is calculated for each of the fuels by Equation 23 below from Reference 2. Table 8 shows the results from calculating f_{st} by Equation 23 for each of the fuels studied in this analysis, in ascending order.

$$f_{st} = \frac{36x + 3y}{103(4x + y)} \quad \text{where the fuel is represented in the form of } C_xH_y \tag{23}$$

Table 8: Stoichiometric Fuel-to-Air Ratios for Fuels for Analysis

Fuel Type	Chemical Formula	f_{st}
Hydrogen	H_2	0.0291
Methane	CH_4	0.0583
Ethane	C_2H_6	0.0624
Hexane	C_6H_{14}	0.0659
Octane	C_8H_{18}	0.0664
JP-7	$C_{12}H_{25}$	0.0674
JP-10	$C_{10}H_{16}$	0.0707

With the h_{PR} and f_{st} established, the one-dimensional flow analysis equations are run repeatedly for a range of freestream Mach numbers to determine the maximum T_3/T_0 possible with supersonic flow maintained throughout the burner, that is, where M_3 and M_4 are both greater than 1. The advantage of using a range of freestream Mach numbers is that if the fuel is not able to maintain supersonic combustion at a T_3/T_0 for Mach 3.50 with practical performance, it will be possible to determine the minimum freestream Mach number at which the fuel can do so.

The ignition temperatures listed in Table 7 must be taken into account to determine the T_3/T_0 required for each fuel to ignite in the airflow at each freestream Mach number. Therefore, the results for the maximum possible T_3/T_0 for each fuel were then compared to the necessary T_3/T_0 to ignite each fuel for each freestream Mach number. The analysis was completed starting with an M_0 of 3.50 and continuing upwards until ignition could be accomplished. Once ignition was reached, the analysis was not continued for higher Mach numbers, as the goal of this project is to reduce the starting Mach number to 3.50, or, if this can not be accomplished, a Mach number that is at least lower than the typical starting Mach number range of Mach 5.0-6.0. A margin was included in these calculations to allow for error by adding 5% to the necessary T_3/T_0 and subtracting 5% from the possible T_3/T_0.

A summary table of the results is provided in Table 9, again in order of descending ignition temperature. Methane is mentioned often as a fuel for a hypersonic cruiser with Mach 6+ cruising speed and hydrogen, as previously discussed, is applicable for Mach 8-10+ applications due of its high energy content. However, neither hydrogen nor methane was chosen as a feasible fuel for the current project, as their lowest starting Mach numbers are 5.50 and 5.35, respectively, therefore providing no ability to lower the starting Mach number. Ethane was not applicable as a feasible fuel either, since its lowest starting Mach number at f_{st} is 5.0. JP-10 is used in missiles and some PDE designs. Though it reduces the starting Mach number at f_{st} to 4.35, it was not the best choice available for this application as there are other fuels which are able to reduce it even further.

JP-7 was developed for the SR-71 [12] and is used for military applications today. It reduces the starting Mach number at f_{st} to 4.3, and was chosen as a candidate fuel due to its wide availability and engine cooling capabilities. Hexane is similar in starting Mach number to JP-7, reducing it to 4.3 as well. However, hexane was not a necessary choice for further pursuit, as its results are similar to JP-7 and is not used as widely. Octane is a widely available fuel and succeeds in reducing the starting Mach number the furthest to 4.25; therefore it was also chosen as a candidate fuel for this project.

Table 9: Summary of Lowest Starting Mach Numbers and Corresponding T_3/T_0 for Analyzed Fuels

Fuel Type	IT (K)	Lowest Starting M_0	T_3/T_0
Hydrogen	845.15	5.50	4.00
Methane	810.15	5.35	3.75
Ethane	745.15	5.00	3.50
JP-10	518.15	4.35	2.50
JP-7	514.15	4.30	2.50
Hexane	498.15	4.30	2.40
Octane	479.15	4.25	2.25

When analyzing the resulting starting Mach numbers displayed in Table 9, it is evident that there is a trend between the ignition temperature of the fuels and the resulting scramjet starting Mach number. Thus, these values are plotted in Figure 7 below. A trend which is nearly linear emerges, making it possible to determine the approximate minimum freestream starting Mach number possible for a fuel when given only its ignition temperature—a useful ability for a preliminary design check. The equation which approximates this is:

$$M_{0,starting} \cong 0.0034IT + 2.6096 \tag{24}$$

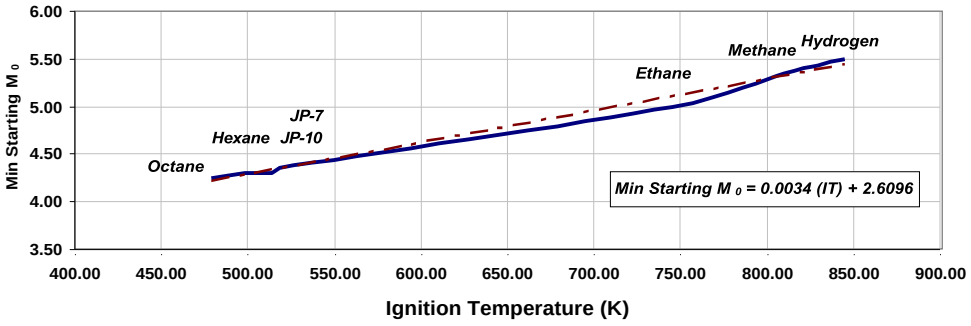

Figure 7: Lowest Possible Scramjet Starting Mach Number versus Ignition Temperature at Stoichiometric Fuel-to-Air Ratios for Several Fuels

The lower the ignition temperature of a fuel, the more the starting Mach number can be reduced. Secondarily, the higher the heat of reaction of a fuel, the better the overall performance of the engine will be.

Turning back to the problem at hand, the fuels which performed the best at stoichiometric fuel-to-air ratios and were the most applicable overall are JP-7 and octane. However, neither fuel reduced the starting Mach number to 3.50. There is still another key design parameter that was explored—varying the fuel-to-air ratio. Before trying to further reduce the starting Mach number though, a decision was first made as to which fuel was better suited for the current project. The following points were important in this decision:

- Octane and JP-7 returned similar results: starting Mach numbers of 4.25 and 4.30, respectively.
- In the SR-71 engine, JP-7 was used in the engine hydraulic system in addition to being the propellant. [12]
- In high Mach number flight in the SR-71, JP-7 served as "a heat sink for the various aircraft and engine accessories which would otherwise overheat at the high temperatures encountered" [12].
- JP-7 contains A-50, which aided in disguising the radar signature of the exhaust plume of SR-71 [12].

In considering the above points, and due to its past military applications, JP-7 stands out as the best fuel for the current project. Though the resulting performance with JP-7 was good, it was necessary to determine whether varying the fuel to air ratio could reduce the starting Mach number to the desired 3.50.

D. Analysis: Variation of Fuel-to-Air Ratio

The stoichiometric fuel-to-air ratio f_{st} is defined by Equation 23. The stoichiometric f is the fuel-to-air ratio which "usually results in the greatest liberation of sensible energy from the breaking of molecular bonds" [2]. In the variation of f, when f is smaller than the f_{st}, the available oxygen is not fully used and when f is larger than the f_{st}, fuel is wasted as not all of it can be burned [2]. Therefore, f_{st} is the ideal upper limit for the fuel-to-air ratio [2]. So, by varying f, combustion is not necessarily ideal. However, the goal of this project is not to produce ideal combustion (though it is always beneficial), but rather to lower the freestream Mach number at which the scramjet can start.

In order to know the limits for the variation of f, the equivalence ratio is used. Defined by Equation 25 below, the equivalence ratio is the ratio of the fuel-to-air ratio used to the stoichiometric fuel-to-air ratio [2].

$$\phi \equiv \frac{f}{f_{st}} \tag{25}$$

Heiser and Pratt state that a general guideline for the equivalence ratio is from 0.2 to 2 for "combustion to occur within a useful timescale" [2]. Therefore, the fuel-to-air ratio has been varied across this range for JP-7 fuel. The variation of the fuel-to-air ratio f across the recommended equivalence ratio range produces the results shown below in Table 10 for JP-7 fuel.

Table 10: Fuel-to-Air Ratios Used for Analysis with JP-7 Fuel and Corresponding Equivalence Ratios

Equiv Ratio	f
1.78	0.12
1.63	0.11
1.48	0.10
1.34	0.09
1.19	0.08
1.04	0.07
0.89	0.06
0.74	0.05
0.59	0.04
0.45	0.03
0.30	0.02

Stream thrust analysis is again applied with a range of freestream Mach numbers from 3.50 to 4.50 and the range of fuel-to-air ratios listed above. Since the limiting factor is the ignition temperature of the fuel, and the T_3/T_0 has been low due to the lower Mach number goal, the maximum possible T_3/T_0 for supersonic combustion to be maintained at each f was determined and recorded. Then, from these results, the minimum possible T_3/T_0 which could ignite the JP-7 fuel was found, as this is obviously necessary for supersonic combustion to even begin. Again, a 10% margin is implemented.

Compiling the data from the stream thrust analysis results and including the lower limit of the required T_3/T_0 for JP-7 fuel to ignite, the design space for a scramjet with JP-7 fuel, plotted against the variation of f, is shown in Figure 8. A linear trendline has been added in the plot, which, upon testing, proves to be highly accurate compared to the one-dimensional flow results. This equation approximates the maximum value of f that can be used with JP-7 fuel while maintaining supersonic combustion and ensuring JP-7 ignition when given a desired starting freestream Mach number. It is:

$$f \cong 0.0543 M_0 - 0.185 \tag{26}$$

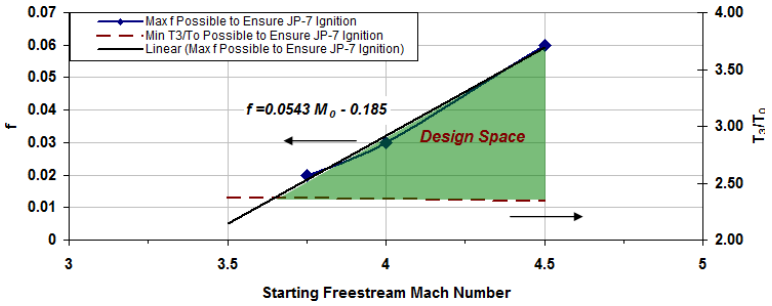

Figure 8: Design Space : Fuel-to-Air Ratio versus Starting Mach Number for JP-7 Fuel; Bounded by Minimum T_3/T_0 Necessary for JP-7 Ignition

It is evident in Figure 8 that the available design space does not extend down to Mach 3.50. Using Equation 26 above, assuming the trend continues linearly, the required fuel-to-air ratio for a scramjet to maintain supersonic combustion at Mach 3.50 would be 0.005. However, if this is entered into the one-dimensional stream thrust equations used for analysis, the combustor entrance temperature (T_3) is still just shy of the required ignition temperature for JP-7 fuel. Therefore, without fuel additives or another way of lowering the ignition temperature of JP-7, a scramjet with a starting Mach number of 3.50 is not possible, according to this one-dimensional flow analysis.

Therefore, as a starting Mach number of 3.50 cannot be accomplished, it is prudent to turn attention to what can. The design space suggests that the lowest possible starting Mach number lies approximately between Mach 3.50 and 3.75. By utilizing the stream thrust analysis equations iteratively, the minimum possible starting freestream Mach number for a scramjet using JP-7 fuel and no additives maintaining supersonic flow is found to be 3.65. Equation 26 yields a similar result with M_0=3.68.

However, at this lowest limit of the design space, there is relatively no room for error. To ensure that the engine does not transition to subsonic combustion, causing a normal shock wave to form in the combustor thereby choking the engine, and to ensure that JP-7 is actually ignited inside of the confines of the combustor, the starting freestream Mach number of the scramjet will be taken to be 4.00. Additionally, this starting Mach number has the ability to

operate with a fuel-to-air ratio of 0.03, which is above the normally stated minimum lean value limit of 0.02 to maintain combustion.

Fuel-to-air ratio variation analysis was also completed for the several fuels that are often considered for scramjet applications for comparison purposes. The resulting design space for each of these fuels can be seen in Figure 9. It is evident from this figure that methane and hydrogen are not able to start at a freestream Mach number lower than 5.00. Also, it appears that octane, though performing slightly better than JP-7 in the fuel selection study at lowering the starting Mach number, cannot achieve a starting M_0=3.50 either, without additives. The individual design space plots for octane, methane, and hydrogen with a variation in fuel-to-air ratio can be found in Reference 6, Appendix B.

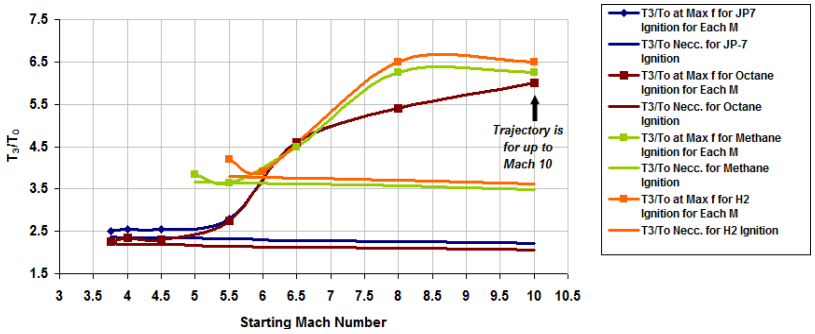

Figure 9: Design Space : T_3/T_0 versus Starting Mach Number for Various Fuels with Variation of Fuel-to-Air Ratio

The trend in Figure 10 below represents the starting Mach number at each fuel's stoichiometric fuel-to-air ratio; all of the analyzed fuels are included. The figure also shows the lowest possible starting M_0 for each fuel across each fuel's allowable equivalence ratio range for *f* in the form of deviation bars.

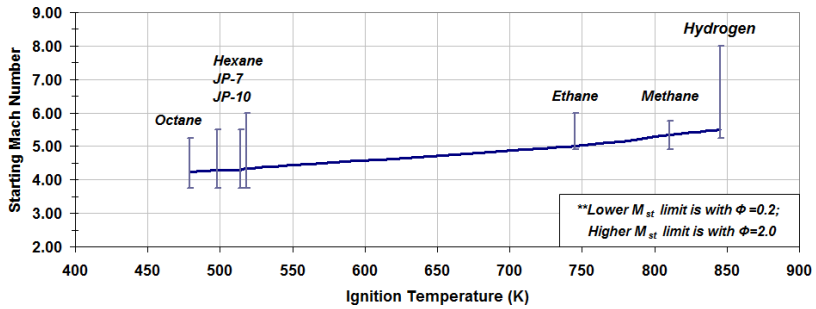

Figure 10: Starting Mach Number as a Function of Ignition Temperature and Fuel-to-Air Ratio

Figure 11 below further emphasizes the point. For the lean fuel-to-air ratio of 0.02, Equations 2 through 22 were repeatedly run for a range of T_3/T_0 at Mach 3.50. For each T_3/T_0, the maximum heat of reaction possible to keep the flow supersonic in the combustor was determined. The results were then plotted in Figure 11 below. A point for each fuel analyzed was plotted at the location where its h_{PR} and minimum T_3/T_0 for ignition intersected. It is evident from this figure that with the lowest fuel-to-air ratio possible, none of the fuels analyzed are able to start the scramjet at a freestream Mach number of 3.50.

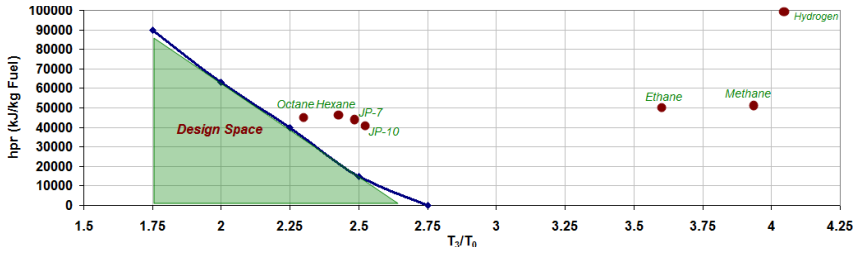

Figure 11: Design Space for Scramjet Start at Mach 3.50: Maximum h_{PR} to Maintain Supersonic Flow in the Combustor as a Function of T_3/T_0 with f=0.02

In conclusion, the analysis has shown the lowest possible starting Mach number of a scramjet engine. With JP-7 fuel and no additives, a scramjet can start at a freestream Mach number of approximately 3.68. This is obviously not as low as the desired Mach 3.50 starting point; however, as it is often said, knowing the boundaries is half of the problem. The design of a scramjet with a starting Mach number of 4.00 is a realistic and readily applicable one, in addition to the fact that it is at least a Mach number below the lower end of the average range of starting Mach number scramjet designs, making it a worthwhile endeavor.

Although it is possible to use a value of f =0.03 at M_0=4.00, the value of 0.02 is used in order to give more of a margin for the combustor entrance temperature to fluctuate and still ensure that ignition of JP-7 begins. A fuel-to-air ratio of 0.02 corresponds to an equivalence ratio of 0.3, which is above the minimum required equivalence ratio (0.2 to 2) for "combustion to occur within a useful timescale" [2]. Although it is near the lean limit for combustion, a value of f =0.02 allows T_3 to decrease by 19% and still ignite JP-7; however, with f =0.03, T_3 can only decrease 8% before reaching the lowest limit possible for JP-7 ignition.

III. Design of a Scramjet with Starting Mach Number of 4.00

A scramjet has been designed to operate from Mach 4 to Mach 10. Though Mach 3.50 would provide more of a margin, a Mach 4.00 starting scramjet is still a possibly feasible choice, as a turbojet engine is capable of providing "thrust from takeoff up to a Mach of 3-4" [3].

Therefore, the benefits of having a lower starting Mach number scramjet would still be possible as a vehicle using this system would only require two propulsion systems, therefore reducing overall vehicle weight and complexity. Mach 10 is still used as the upper limit for the design of the flowpath as JP-7, a hydrocarbon fuel, will be used. Waltrup states that the "maximum freestream Mach number of a hydrocarbon-fueled scramjet-powered vehicle flying at 47.88 MN/m^2 trajectory would be between Mach 9 and 10" [13]. Therefore, in order to ascertain the overall vehicle performance of a Mach 4.00 starting scramjet across the entire possible performance range, Mach 10 is used as the upper limit of the flight path.

This chapter details the design process for the flowpath of a scramjet with a starting M_0=4.00, T_3/T_0=2.80, and f=0.02. The design process includes the design of the compression system, isolator, combustion system, and expansion system. The design of the scramjet is undertaken in the order in which air proceeds in the flowpath-compression, combustion, and expansion; the following subsections will therefore be divided accordingly.

A. Design: Compression System and Inlet

The goal of the compression system in a scramjet engine is to "provide the desired cycle static temperature ratio (T_3/T_0) over the entire range of vehicle operation in a controllable and reliable manner with minimum aerodynamic losses i.e., maximum compression efficiency or minimum entropy increase" [2]. This compression, for the one-dimensional analysis used throughout this project, relies on oblique shock waves. Normal shock wave compression is reserved for ramjets as it is able to offer "reasonable performance for $0 < M_0 < 3$," whereas for Mach numbers greater than 3, the "normal shock losses become unacceptably high and oblique shock compression becomes necessary" [2].

There are three options for the application of oblique shock waves in a scramjet: internal, external, and mixed internal and external compression [2]. As internal compression is highly complex in design and this project is a preliminary analysis based on one-dimensional flow and integration issues are not yet visible, mixed internal and external compression has been used as it allows for a cowl that is parallel to the freestream flow.

Before detailing the method of the compression system design, it should be noted that the compression system is important in the determination of the performance of the overall engine, as the airflow which exits the compression

system feeds directly into the burner. Due to the complex nature of flow in a compression system, CFD analysis or physical experiments are often needed [2]. However, for a preliminary study, an estimation will suffice. Therefore, the following assumptions are made for the compression system design process, as taken from Reference 2:

1. One-dimensional flow; boundary layer is represented only by its average effect on flow properties.
2. Air is represented as a calorically perfect gas.
3. Heat transfer to or from the wall will be neglected.

With these assumptions, inviscid compression system analysis is used to design the compression system. For this project, the tool HAP(GasTables) [2] was used to calculate the performance of the resulting compression system. This tool accompanies the Reference 2 text and calculates the compression system's oblique shock wave configuration for the given number of oblique shock waves, the freestream Mach number, and the static cycle temperature ratio specified [2]. The output is the resulting properties at the exit of the compression system (Station 2), the required turning angle for each shock wave to turn the flow through to accomplish the overall required compression, the static pressure ratio, the adiabatic compression efficiency, and the kinetic energy efficiency [2, 14]. HAP(GasTables) works by calculating "special families" of hypersonic compression systems, which are "characterized by the cardinal number of oblique shock waves available to produce a specified cycle static temperature ratio at a specified Mach number" and in the cases when more than one shock wave is specified, "all oblique shock waves must provide equal amounts of geometric turning of the flow" [2]; the disadvantage is that the flow is not turned back to the axial direction. The compression sequence in this tool is assumed to begin at the leading edge of the vehicle [2].

A "special family" can be designed by using HAP(GasTables) for as many cases as necessary by inputting M_0, T_3/T_0, γ_c, and the number of desired oblique shock waves. The number of oblique shock waves has a direct impact on the compression efficiency (η_c); a good estimate of this correlation can be seen in Figure 12 below. It is from this figure that an educated guess can be made as to how many shock waves are necessary based on the M_0, T_3/T_0, and the desired compression efficiency. It should be noted that the higher the number of oblique shock waves, the longer the compression system will be. Also, with more oblique shocks, more off-design complications will exist. With this information input into HAP(GasTables), the tool then calculates the properties of the flow (M, T/T_0, p/p_0, A/A_0, Pt/Pt_0, $(s-s_0)/C_p$) after each oblique shock wave using inviscid oblique shock theory. It is from these performance measures that the determination can be made on whether the resulting compression system of oblique shocks will suffice, or rather HAP(GasTables) should be run again until the best compression system is designed.

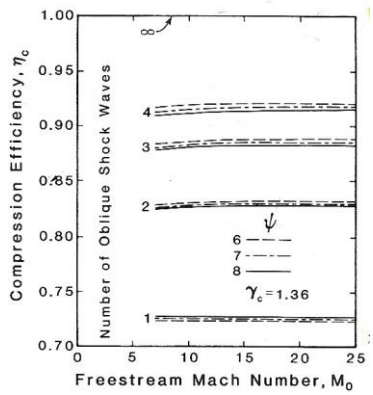

Figure 12: Adiabatic Compression Efficiency (η_c) Correlated to M_0 , T_3/T_0, and Number of Oblique Shock Waves [2]

In order to determine whether the inviscid assumption could be made without a large impact on the outcome, the results with boundary layer friction were calculated and compared to the inviscid results determined from HAP(GasTables) by virtue of a two-step process that compares the flow properties resulting from each method for the design case. Reference 2 states that the range for the dimensionless boundary layer skin friction quantity—$(C_f/2)(A_w/A_3)$—is approximately 0.01 to 0.05, with the "most likely value" being 0.02 [2]. Therefore, using the value of 0.02, the two-step comparison returned a maximum difference of only 2.9% across the Station 2 flow properties in comparison to the inviscid results. This is consistent with the statement made by Heiser and Pratt that "boundary-layer friction should do little to diminish overall scramjet performance for freestream Mach numbers up

to about 10 or 15" [2]. Thus, the compression system calculations for the design of the scramjet with a starting Mach number of 4.00 were completed with the HAP(GasTables) inviscid oblique shock wave tool.

The input values to begin the design process of the compression system had to be determined first. The values of M_0 and T_3/T_0 were determined as a result of the analysis explained in Chapter 2. The value of γ_c is a constant also used in the analysis. The number of oblique shocks was the only remaining design constraint to be determined, and was found by analyzing Figure 12. As the general rule of thumb assumption for η_c is 0.90 [2], it is evident from the figure that achieving at least this efficiency with a T_3/T_0=2.80 requires at least three oblique shock waves. HAP(GasTables) was run for both the three and four oblique shock wave cases. These results can be seen below in Table 11 and 12, respectively.

Table 11: Results of Inviscid Compression System Design with Three Oblique Shocks

Input						
M_0	4					
T_3/T_0	2.8					
Number of OS	3					
γ_c	1.362					
Flow Properties to Determine Station 2 Values			**Resulting Compression System Properties**			
p_0	4275	Pa	**delta**	16.9499	deg	
T_0	218.22	K	$p_{t3}/p_{t0}=\pi_c$	0.6111		
C_{pc}	1090	J/kgK	n_c	0.9223		
V_0	1184.56	m/s	n_{ke}	0.9517		
Flow Properties After Each Oblique Shock						
O.S. Number	**M**	**T/T_0**	**p/p_0**	**A/A_0**	**p_t/p_{t0}**	**$(s-s_0)/C_p$**
1	2.8551	1.5739	4.1260	0.4260	0.7489	0.0768
2	2.0903	2.1755	12.2165	0.2310	0.6560	0.1120
3	1.4706	2.8000	29.4134	0.1547	0.6111	0.1309
Flow Properties at Compression System Exit						
		p_2	125742.285	Pa		
		T_2	611.016	K		
		V_2	739.518163	m/s		
		M_2	1.4706			

Table 12: Results of Inviscid Compression System Design with Four Oblique Shocks

Input						
M_0	4					
T_3/T_0	2.8					
Number of OS	4					
γ_c	1.362					
Flow Properties to Determine Station 2 Values			**Resulting Compression System Properties**			
p_0	4275	Pa	**delta**	13.3082	deg	
T_0	218.22	K	$p_{t3}/p_{t0}=\pi_c$	0.721		
C_{pc}	1090	J/kgK	n_c	0.9495		
V_0	1184.56	m/s	n_{ke}	0.9686		
Flow Properties After Each Oblique Shock						
O.S. Number	**M**	**T/T_0**	**p/p_0**	**A/A_0**	**p_t/p_{t0}**	**$(s-s_0)/C_p$**
1	3.1063	1.4186	3.1775	0.4827	0.8526	0.0424
2	2.4565	1.8622	8.1162	0.2738	0.7824	0.0652
3	1.9350	2.3222	17.7187	0.1778	0.7443	0.0785
4	1.4706	2.8000	34.6985	0.1312	0.7210	0.0870
Flow Properties at Compression System Exit						
		p_2	148336.0875	Pa		
		T_2	611.016	K		
		V_2	739.5181631	m/s		
		M_2	1.4706			

As can be seen in the comparison of the above two tables, the four-shock system returned overall better results. There is less pressure loss, as evidenced by the 0.11 increase in π_c, and in the fact that the compression efficiency is nearly 3% higher than the three-shock system. Therefore, the four-shock system was used as the final compression system design, with the first three shocks taking place external to the engine and the final shock occurring just inside of the engine to turn the flow upward a value of delta, to bring it closer to parallel to the axial direction. A shock cancellation surface is required inside the engine.

B. Design: Combustion System

Though many of these been advanced since 1958, Weber and McKay's summary description of supersonic combustion applies even today: "It is necessary to capture a stream tube of supersonic air, inject fuel, achieve a fairly uniform mixture of fuel and air, and carry out the combustion process—all within a reasonable length, and preferably without causing a normal shock within the engine" [2, 15].

In order to begin the theory behind designing a burner for a scramjet, it is first necessary to define the axial locations of the geometry that will be dealt with. Corresponding to previously designated station numbering, Figure 13 below displays the details of the combustion system station designations.

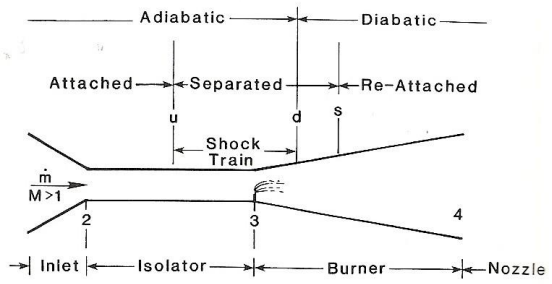

Figure 13: Combustion System Station Designations [2]

As depicted in Figure 13, Station 2 is the entrance to the isolator, Station 3 is the entrance to the burner, and Station 4 is the exit from the burner and entrance to the expansion nozzle. Stations *u* and *d* are the upstream and downstream limits of a "positive or adverse axial pressure gradient, respectively" [2]. Station *s* is the upstream limit of the "negative or favorable pressure gradient which extends through the remainder of the burner and right on through the expansion system" [2] and is also the location of the lowest Mach number in the entire combustion system [2].

The combustion system design method includes two main components for its analysis: the isolator and the burner. The isolator is generally considered to be a part of the compression system, but it is included here in the design of the combustion system due to the important role the isolator design plays on the combustion system design. The primary function of the isolator is to prevent inlet unstart, by "providing sufficient additional adiabatic compression above its entry pressure p_2 to match or support whatever back pressure p_3 the burner may impress upon it" [2]. The isolator does not have a direct interaction with the flow in the burner unless there is flow separation caused by "thermal occlusion unrelieved by area expansion" [2], causing a back pressure on the isolator. The burner is the active component of the combustion system which injects the airflow with fuel, ensures adequate time for mixing and ignition, and passes off the resulting flow to the expansion system to generate thrust.

One-dimensional flow analysis was also employed for the design of the combustion system by utilizing the Design tool of the HAP(Burner) code [2, 14]. The authors of the code cite Shapiro [16, 17] as their key reference.

The burner for the current scramjet project is designed for constant pressure at a freestream Mach number of 4.00. For the constant-pressure burner, there are two possibilities for the isolator-burner interaction.

- *Scramjet with shock-free isolator.* In this case, there is no pressure feedback from the burner to the isolator, assuming frictionless flow [2]. Therefore, there is no interaction between the two components as a shock system is not needed in the isolator to equalize backpressure from the burner. This is the least complex, and therefore, optimal design.
- *Scramjet with oblique shock train.* In this system, there is a pressure feedback from the burner which is kept from propagating upstream to the inlet, thereby inlet unstart is prevented, by an oblique shock train in the isolator [2].

The isolator type was also determined through the use of the Design tool in the HAP(Burner) software [2]. The required inputs for this program are: the state and Mach number of air entering the combustion system (M_2, T_2, u_2, p_2, R_b, γ_c), the length and divergence angle of a planar combustor geometry (x, A/A_2, θ/H, H) and an estimate of axial distribution of total temperature (θ, x_i, η_b/h_{PR}) [14]. The program then determines "whether or not a solution is possible for the given inputs, and if possible, calculates the axial variation of static and total properties within the combustion system, including effects of internal flow separation and choking due to thermal occlusion" [14].

The source and/or method for determining the inputs required for the program are discussed in turn below:

- *State and Mach Number of Air Entering the Combustion System (M_2, T_2, u_2, p_2, R_b, γ_c).* The quantities required from Station 2 were determined from the compression system design in the preceding

subsection. These are shown in the bottom rows of Table 12. The values of R for the burner and γ for the compression system are constants and can be found in Table 13.

- *Length and divergence angle of a planar combustor geometry (x, A/A_2, θ/H, H).* The default values for x that are in HAP(Burner) were used. After the design is complete, the default x values were then added to the length of the compression system, thereby keeping the same axial variation in the combustion system. H was kept at the default value unless changes were needed during the process. A/A_2 and θ/H were varied systematically to determine the necessary values to keep the pressure constant in the burner and to provide for the necessary Station 3 and 4 values.
- *Estimate of axial distribution of total temperature (θ, x_i, $\eta_b f h_{PR}$).* The value of θ was varied systematically to determine the necessary value to keep the pressure constant in the burner and to provide for the necessary Station 3 and 4 values. The value of x_i was assumed to occur at the burner entrance, and therefore the default value of x_i was used. The value of $\eta_b f h_{PR}$ is a constant, defined by the product of the burner efficiency, fuel-to-air ratio of 0.02, and the heat of reaction of JP-7. The burner efficiency was assumed at 0.90 as Reference 2 assumes.

The values that served as the desired result for Stations 3 and 4 during this process were determined from dividing the values of pressure, temperature, and velocity at Stations 3 and 4 (determined by the preliminary results of the one-dimensional flow equations) by the corresponding values of the same at Station 2. These results, as well as M_3 and M_4 could then be compared to the results produced by HAP(Burner) for the same parameters; the systematically varied parameters of A/A_2, θ, and θ/H were adjusted accordingly until the results were roughly equivalent. The flow parameters for Stations 3 and 4 were determined from the results of applying Equations 2 through 22 in the spreadsheet built for this project with the same input as detailed in Chapter 2, except for η_c which is now 0.9495, due to the design of the compression system in the previous subsection. Table 13 summarizes the input values used in the HAP(Burner) code. Table 14 shows the desired Station 3 and 4 values which were used as the goal as the program was repeated. Note that the values of p_3/p_2 and p_4/p_2 are equal, as an ideal constant-pressure burner should have.

Table 13: Input Values for the HAP(Burner) Program for Combustion System Design

Flow Properties at Station 2		
M_2	1.47	
T_2	611.02	K
V_2	739.52	m/s
p_2	148.3361	kPa
R_b	289.30	J/kg-K
γ_c	1.238	
Isolator/Combustor Geometry		
x(2, 3, 3p, 4)	(0, 0.914, 0.914, 1.829)	m
A/A_2(2, 3, 3p, 4)	(1, 1, 1, 1.8-2.5)	
θ/H	Vary: 0.01-0.03	
H	0.152	m
Axial Heat Addition Parameters		
θ	Vary: 1 to 10	
x_i	0.914	m
$\eta_b f h_{PR}$	790.263	kJ/kg

Table 14: Station 3 and 4 Flow Parameters: Serves as Check for Desired Output from HAP(Burner)

	M	p/p_2	u/u_2	T/T_2
Station 3	1.51	1.005	1.0000	1.0000
Station 4	1.09	1.005	0.9411	1.8568

Therefore, with the inputs as listed in Table 13, HAP(Burner) was run repeatedly until the values shown in Table 14 were met or matched as closely as possible and a shock-free isolator system was obtained. This process was done eleven times before all parameters were matched as closely as possible. The result includes a shock-free isolator. Table 15 below shows the final Station 3 and 4 flow parameters which are comparable to the desired results shown in Table 14.

Table 15: Final Station 3 and 4 Flow Parameters

	M	p/p_2	u/u_2	T/T_2
Station 3	1.581	1.000	1.0000	1.0000
Station 4	1.16	1.000	1.0000	1.8590

The iterations included four variations of the three-shock compression system shown in Table 11; the rest of the variations were done with the four-shock system which was selected in the previous subsection as the compression system of choice. The three-shock compression system was varied here to ensure that the four-shock system was indeed the best selection. It is important that the burner design code is run before deciding on a final compression system to ensure that the required burner results can be obtained with the compression system selected.

C. Design: Expansion System

As Heiser and Pratt state, "the function of the expansion component is to produce thrust" [2]. The expansion system begins at Station 4 and ends at Station 10, where, ideally, $p_{10}/p_0=1$. However, scramjet expansion systems often operate underexpanded, that is $p_{10}/p_0>1$ [2]. Operating underexpanded provides a benefit by decreasing the overall length of the expansion system, thereby decreasing the overall length of the engine.

Despite the fact that the exhaust flow is far from one-dimensional, it can still be approximated to a degree through one-dimensional analysis, as much of the flow leaving the engine lies in the axial direction [2]. Additionally, as the goal of the current study was to lower the starting Mach number of a scramjet, the expansion system was not the primary component of interest since it is not a principal determinant of the starting freestream Mach number of the engine.

In the design of the expansion system, an ideal nozzle ($p_{10}/p_0=1$) was assumed for the Mach 4.00 on-design condition as well as for the off-design conditions for comparison purposes of the resulting performance characteristics. Therefore, the assumption was effectively that of a variable geometry expansion system. Such a system is not a practical one; however, as Figure 14 below shows, whether or not the nozzle is designed practically (that is, a non-ideal, non-variable nozzle) does not make a large difference in the overall performance for the one-dimensional case, as the curve begins to level off early in the expansion process. Heiser and Pratt state that a "partial expansion can indeed recover most of the available thrust" [2].

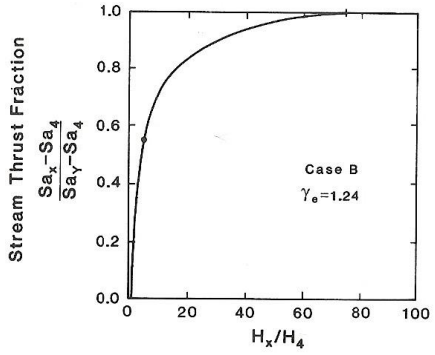

Figure 14: Stream Thrust Fraction as a Function of Local Height to Entry Height of the Expansion System [2]

With this assumption in place, the expansion system was calculated and thereby designed for each Mach number with the one-dimensional flow analysis equations as a Single Expansion Ramp Nozzle (SERN) [18]. These equations were used for the expansion component, with the results from HAP(Burner) for the flow parameters at Station 4 for each Mach number used as input. The expansion system was designed for each Mach number using the one-dimensional flow analysis equations for the expansion component with the ideal expansion assumption of $p_{10}/p_0=1$. A Single Expansion Ramp Nozzle (SERN) was used with an assumed expansion angle value of 20 degrees [18].

This analysis utilized Equations 12-15, with the results from HAP(Burner) for the flow parameters at Station 4 for each Mach number used as input. The resulting performance was then determined, as before, using Equations 16-22.

The method to determine the expansion system values was to change the input sources for M_4, T_4, V_4, and p_4 in Equations 12-15 (expansion component equations) to the actual HAP(Burner) output instead of using the results of Equations 8-11 (combustor component equations) in the spreadsheet described previously which calculates the one-dimensional flow analysis. The result was output that includes the results of the design of the compression and combustion systems which is used for the design of the expansion component and in the calculation of the overall engine exit parameters. The two-dimensional schematic illustrating the resulting expansion system can be found in the next chapter as a part of the overall scramjet design schematic. Chapter 4 will also detail the performance of the final scramjet, for both on- and off-design conditions; the expansion system output values can be seen in Table 16 in that chapter for the on-design case designed here.

IV. Resulting Scramjet Engine Design and Performance with a Starting Mach Number of 4.00

A. Scramjet Engine Design and Results

Figure 15 shows the results of plotting the height as a function of axial location: the two-dimensional view of the overall scramjet designed for the design point at a starting M_0= 4.00 with JP-7 fuel.

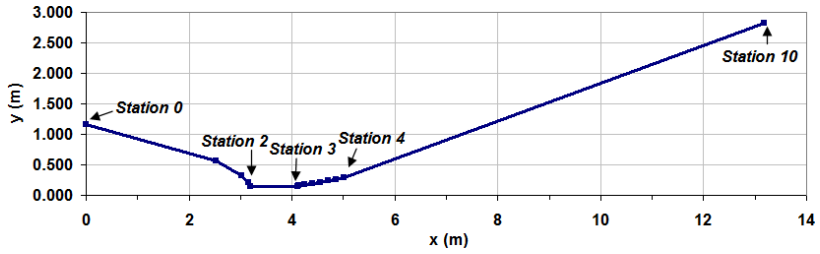

Figure 15: Two-Dimensional Schematic of the Overall Scramjet Designed for Mach 4.00 Start

The on-design performance of the scramjet is evaluated at M_0=4.00, the freestream Mach number at which the engine starts and for which the engine is designed.

Table 16: On-Design Performance Calculation: Component Parameters for Scramjet Designed for Mach 4.00 Start

OUTPUT		
Compression Component (0 to 3)		
Sa_0	1237.855	
T_3	611.016	K
V_3	739.518	m/s
M_3	1.581	
Sa_3	978.548	
p_3/p_0	34.866	
p_3	148306.420	Pa
A_3/A_0	0.129	
Combustion Component (3 to 4)–Constant Pressure Combustion		
V_4	739.518	m/s
M_4	1.160	
T_4	1135.879	K
A_4/A_3	1.896	
Either Constant Pressure or Constant Area Combustion		
Sa_4	1183.875	
Expansion Component (4 to 10)		
p_4/p_0	34.678	
T_{10}	631.812	K
V_{10}	1438.461	m/s
M_{10}	3.024	
Sa_{10}	1565.530	
A_{10}/A_0	2.432	

Table 17: On-Design Performance Results for Scramjet Designed for Mach 4.00 Start

Engine Performance Measures		
F/m_o	282.671	N-s/kgA
S	7.075E-05	kg F/s-N
I_{sp}	1440.73	s
n_o	0.381	
n_{th}	0.403	
n_p	0.947	
T_3	611.02	
T_4	1135.88	
T_{10}	631.81	
M_3	1.58	
M_4	1.16	
M_{10}	3.02	

The H-K diagram for the scramjet at the on-design condition is shown in Figure 16 below. As can be seen in this figure, at Station 0, the freestream air is decelerated and compressed through the four oblique shock waves of the inlet compression system up to the isolator inlet at Station 2, resulting in a loss in K and an increase in H. Stations 2 and 3 occur at the same H and K, since the isolator is shock-free. Inside the combustor, as the air is heated to ignite the fuel, the pressure is constant for the on-design case, keeping K constant as H steadily increases from Station 3 to Station 4. This results in constant velocity throughout the burner as well. After exiting the combustor, the air is then expanded and accelerated in the expansion system from Station 4 to Station 10 to freestream conditions. The Mach number at the exit can never equal the freestream Mach number due to total pressure loss through the engine, but as long as the Mach number is large enough at the exit for K_{10} and V_{10} to exceed K_0 and V_0 respectively, net thrust is generated [2]. It is evident in Figure 16 that this is indeed the case for the scramjet designed here.

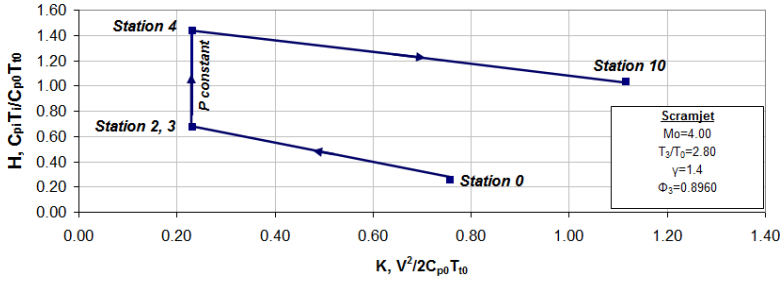

Figure 16: H-K Diagram for On-Design Performance Results for Scramjet Designed for Mach 4.00 Start

Although the determination of the on-design performance is important, perhaps equally as important is the calculation of the performance during flight when the scramjet must operate at off-design Mach numbers. After all, if an engine is only able or worthwhile to operate at one flight Mach number, there is not much application for it. As the goal of this project was to design a scramjet with a lowered starting Mach number, Mach 4.00 is the design case. The remaining Mach numbers of operation up to Mach 10 are then operating in an off-design condition.

Thus, the off-design performance at Mach numbers 5, 6, 8, and 10 was determined and subsequently compared to the off-design performance of a scramjet designed for start and operation at Mach 5.00 (a value in the range of typical scramjet starting Mach numbers), as well as scramjets designed for on-design operation at each respective Mach number with a starting Mach number of Mach 5.00.

Table 18: Off-Design Performance Results for Mach Numbers of 5, 6, 8, 10 Including Mach 4.00 On-Design Data for Comparison

M	Isp (s)	F/m_0(N-s/kgA)	S (kg F/s-N)	η_o	η_{th}	η_p	T_0 (K)	T_3 (K)	T_4 (K)	T_{10} (K)	M_3	M_4	M_{10}	$(H_{10}-H_0)/H_{10}$	$(K_{10}-K_0)/K_{10}$
4	1440.73	282.67	7.08E-05	0.38	0.40	0.95	218.22	611.02	1135.88	631.81	1.58	1.16	3.02	75%	32%
5	1393.77	273.46	7.31E-05	0.46	0.47	0.98	221.09	808.23	1291.55	677.24	1.78	1.50	3.51	76%	26%
6	1301.42	255.34	7.83E-05	0.52	0.51	1.02	223.47	986.68	1443.51	709.57	2.06	1.82	3.99	77%	20%
8	1138.20	223.31	8.96E-05	0.61	0.57	1.09	227.26	1403.04	1798.69	793.93	2.48	2.33	4.86	79%	13%
10	992.98	194.82	1.03E-04	0.68	0.58	1.17	233.16	1919.66	2240.24	908.97	2.80	2.73	5.59	81%	8%

Figure 17 below displays the results of specific impulse and specific thrust across the trajectory; therefore, this trend includes both the on-design performance results for these values at M_0=4.00 as well as the off-design results for M_0=5, 6, 8, and 10.

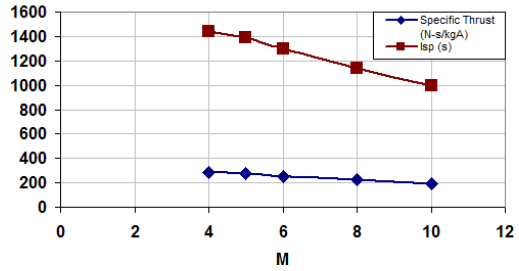

Figure 17: Scramjet Performance Results: I_{sp} and $F \dot{m}_0$ Across Trajectory

As expected, the best performance for both I_{sp} and $F \dot{m}_0$ occurs at M_0=4.00 and declines as the freestream Mach number increases, as the operation point is getting farther away from the on-design condition of the scramjet. Figure 18 displays the results of the variation of the efficiency values across the trajectory.

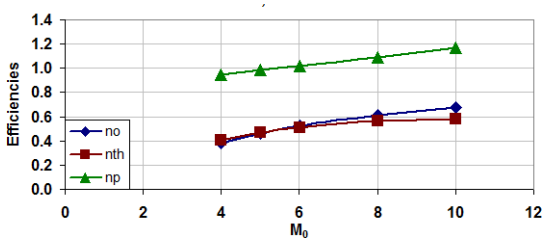

Figure 18: Scramjet Performance Results: η_0, η_{th}, and η_p Across Trajectory

Figure 19 below displays the difference from engine entrance to exit in H and K for each freestream Mach number that was analyzed across the trajectory. As the figure shows, with increasing Mach number, the gain in H and K decreases; this is also a result of the engine design Mach number being 4.00.

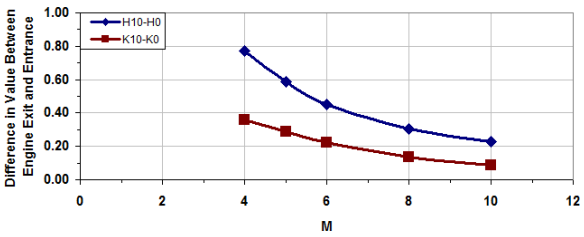

Figure 19: Scramjet Performance Results: Difference from Engine Entrance to Exit in H and K for Each Mach Number

Figure 20 displays the trend of specific fuel consumption across the trajectory, calculated for each freestream Mach number analyzed.

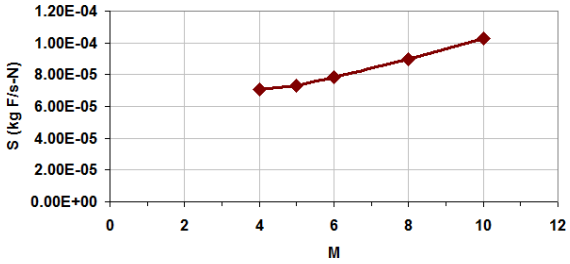

Figure 20: Scramjet Performance Results: Specific Fuel Consumption Across Trajectory

Figures 21 through 25 compare all of the performance values obtained. These include: the on-design performance at Mach 4.00 and the off-design performance at Mach 5, 6, 8, and 10 in the Mach 4.00 scramjet; the on-design performance at Mach 5.00 and the off-design performance at Mach 6, 8, and 10 in the Mach 5.00 scramjet; and the on-design performance obtained for the scramjets designed for operation at each of the other respective Mach numbers (Mach 6, 8, and 10.) The on-design results for the Mach 5, 6, 8, and 10 engines were obtained through individual designs and calculations of results for each Mach number engine as detailed previously for the Mach 4 engine.

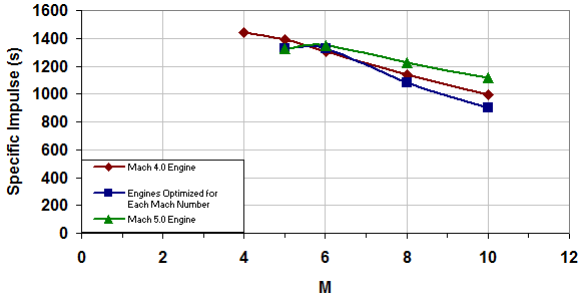

Figure 21: I_{sp} Values for On- and Off-Design Performance of Mach 4 and 5 Designed Engines and for On-Design Performance of Mach 6, 8, and 10 Engines

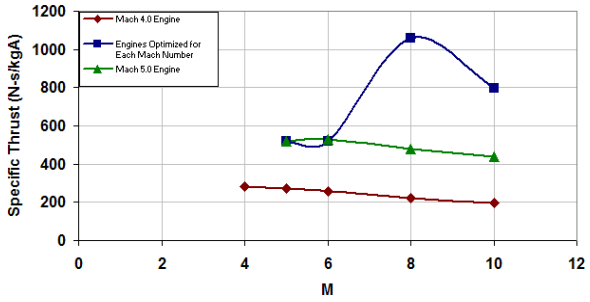

Figure 22: $\frac{F}{\dot{m}_0}$ Values for On- and Off-Design Performance of Mach 4 and 5 Designed Engines and for On-Design Performance of Mach 6, 8, and 10 Engines

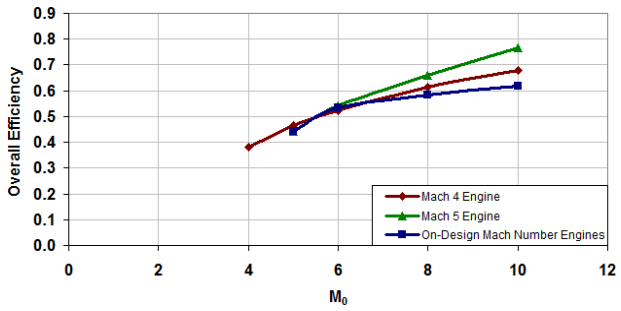

Figure 23: Overall Efficiency Values for On- and Off-Design Performance of Mach 4 and 5 Designed Engines and for On-Design Performance of Mach 6, 8, and 10 Engines

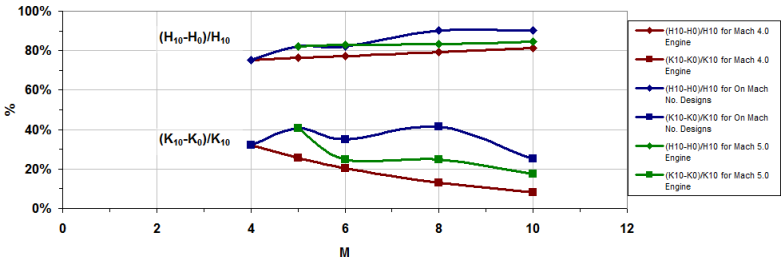

Figure 24: Values of $(K_{10}-K_0)/K_{10}$ and $(H_{10}-H_0)/H_{10}$ for Mach 4 and 5 Designed Engines and for On-Design Performance of Mach 6, 8, and 10 Engines

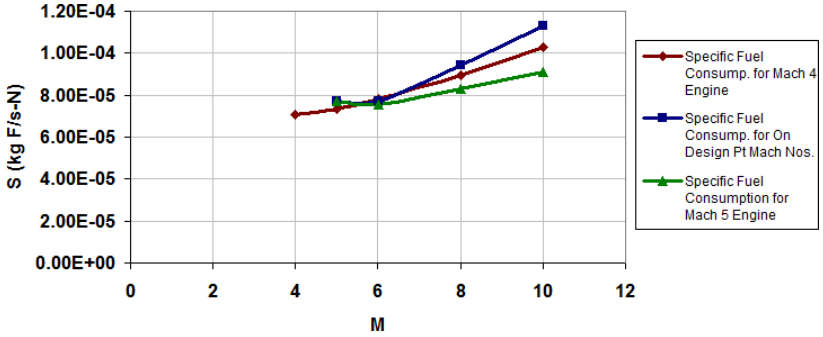

Figure 25: Specific Fuel Consumption for Mach 4 and 5 Designed Engines and for On-Design Performance of Mach 6, 8, and 10 Engines

B. Discussion of Results

The on-design performance investigation (operation at Mach 4.00) resulted in performance values that are acceptable if a lowered starting Mach number is the desired goal. If the purpose of a scramjet to be designed is to achieve the highest efficiency and performance values possible, then this design is not the best choice. The specific impulse of the engine designed is respectable at 1440.73s, especially when considering that the classical I_{sp} versus Mach number plot estimates that the scramjet maximum I_{sp} capability with hydrocarbon fuels is around 1500s as shown below in Figure 26 and when considering that hydrocarbon scramjets have been estimated to be capable of a specific impulse of about 1000 seconds at Mach 6 [19, 20].

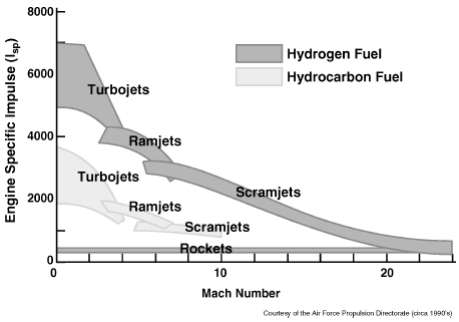

Figure 26: I_{sp} Versus Mach Number Plot for Various Engine Types [3]

However, the high performance for I_{sp} of the Mach 4.00 designed scramjet comes at a cost in specific thrust. As the fuel-to-air ratio is decreased, the specific thrust decreases and the specific impulse increases. As a very low fuel-to-air ratio, such as 0.02 for the case of the Mach 4.00 engine designed in this paper, is needed to start the engine at a low Mach number, specific thrust suffers. Though the specific thrust is not extremely high, the H-K diagram generated and shown in Figure 16 for on-design performance of the Mach 4.00 engine displays that the engine still generates net thrust. This assures that a scramjet with a starting Mach number of 4.00 is possible.

For the off-design performance generated in this chapter of the Mach 4.00 designed engine, the results are intuitive. As the Mach number increases, that is, as the Mach number gets farther and farther away from the design point of Mach 4.00, the specific thrust and specific impulse decrease in an almost linear fashion, with the specific impulse dropping off much more steeply with Mach number than the specific thrust. This trend is also true for the performance comparison case of the Mach 5.00 designed engine at the same off-design Mach numbers. However, overall the Mach 5.00 designed engine returns higher performance values. This is primarily due to the fact that the engine starts at a Mach number closer to the off-design points evaluated.

Conversely, with an increase in Mach number, the overall efficiency increases as well, since it is related directly to velocity; the velocity increases at a faster rate than the specific fuel consumption increases. If the reverse were true, the overall efficiency would decrease steadily with increasing Mach number.

The specific fuel consumption increases with Mach number, as expected, due to the higher velocity (and thus, higher required thrust) of the flow that requires a higher overall quantity of fuel to keep the fuel-to-air ratio steady.

Comparing the relative increase of H and K for each of the cases tested shows that as Mach number increases, the value of H also increases while the value of K decreases. The overall gain in percentage is the highest in H and K for the on-design Mach number engine cases, with the off-design performance for the Mach 5.00 engine consistently being in second, and the gain in H and K of the off-design performance of the Mach 4.00 engine being the lowest of the three trends. This is primarily due to the increased velocity of the two cases with the highest overall gains.

A particularly revealing example of the opposite relationship specific thrust and specific impulse have in relation to the fuel-to-air ratio can be seen in Figures 21 and 22 for the on-design performance evaluation of the Mach 5, 6, 8, and 10 scramjets. As the design Mach number increases, in general the selected fuel-to-air ratio increases as well, due to it providing the best tradeoff between specific impulse and specific thrust. However, as these figures show, the overall trend of specific impulse is decreasing with Mach number, while the overall trend of specific thrust increases. In fact, the trends for specific impulse and specific thrust are relative opposites of each other; as one increases, the other decreases. This is a visual example of the effect that the chosen fuel-to-air ratio has on the design of a scramjet. This insight is especially important when considering the design of a scramjet with a lowered starting Mach number, which therefore requires a lower fuel-to-air ratio to keep the flow supersonic throughout the combustor.

The performance parameters and comparisons generated in this chapter help provide the needed information for the determination of the impact that transitioning to scramjet power at a lower Mach number has on the overall performance.

V. Conclusions

The purpose of this project was to determine whether the freestream starting Mach number of a scramjet can be lowered to 3.50 while performance is maintained in the same flowpath at the higher, off-design Mach numbers and,

if so, to define how it could be accomplished. If the goal is not possible, it was necessary to determine what the constraints are that prevent it and to define the lowest possible starting Mach number.

The purposes of this project were accomplished. By successively analyzing the driving parameters influencing the starting Mach number and applying the necessary theory and equations, it has been determined that obtaining a scramjet starting Mach number of 3.50, without fuel additives or another method of lowering the fuel ignition temperature, is not currently possible with any of the fuels analyzed.

This analysis has determined that in order for a scramjet to start at a Mach number of 3.50, a fuel with a lower heat of reaction and a lower ignition temperature (naturally or with the use of additives) than those analyzed here must be used; these are the key constraints on the ability of the scramjet to start at Mach 3.50. In Figure 27 below, obtained from applying the freestream temperature at the Mach 3.50 condition for a constant q trajectory of 47,880 N/m^2 to Figure 11, for a given ignition temperature of a given fuel, the fuel's heat of reaction value must lay below the line or supersonic combustion will not be maintained.

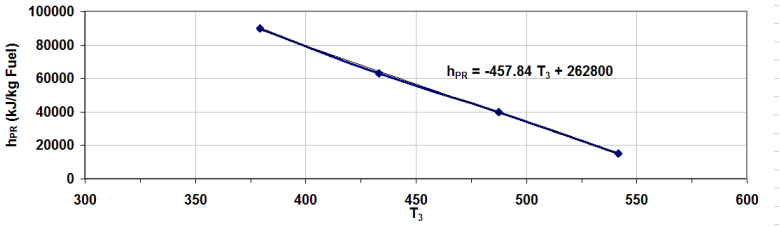

Figure 27: Maximum Heat of Reaction for Mach 3.50 Supersonic Combustion to be Maintained as a Function of Combustor Entrance Temperature (Same as Required Ignition Temperature) at *f*=0.02

With JP-7 fuel and no additives, it has been determined that a scramjet can start at a freestream Mach number of approximately 3.68. However, this leaves relatively no margin for error. The design of a scramjet with a starting Mach number of 4.00 has been shown instead to be a realistic and readily applicable case, and is at least a Mach number below the lower end of the average range of starting Mach number scramjet designs. Therefore, a scramjet with a starting Mach number of 4.00 was designed. Performance results were determined and demonstrate promise, as net thrust is shown to be produced and an impressive specific impulse has resulted.

As discussed previously, Fry states that a turbojet engine can provide for thrust from takeoff to a speed of Mach 3 or 4 [3]. Therefore, if the scramjet designed in this paper were applied to a hypersonic cruiser it could presumably allow for a reduction in total propulsion systems needed.

Acknowledgments

The authors would like to gratefully acknowledge the support and encouragement received from Dr. K.SIVAN, Chairman, ISRO towards the preparation of this book, without which, the book would not have reached the present form.

References

The authors offer their very special thanks to Dr. V. Jayaraman, Prof. J. N. Goswami, Prof. N. Bhandari, Shri. M. Annadurai, Shri. S. K. Shivakumar, Dr. Christian Erd, Prof. R. Sridharan, Shri. A. S. Kiran Kumar, Dr. P. Sreekumar, Shri. T. Parimalarangan, Shri. V. Sundararamaiah, Shri. S. Krishnamurthy, Shri. B.R. Guruprasad, Dr. R. Nanda Kumar, and Ms. Shyama Narendranath for critically reviewing the contents of the book and providing comments and suggestions.

Thanks are also due to Ms. S. Megala for helping in finalising this project review paper.

1. D.satpati and p.v.venkitakrisnan Doubt study of meteorites and their impacts on earth in pslv f 5,8(2) (2018), 240-249. (Atlantis Press and Taylor and Francis) (SCIE)(I.F- 1.151)

2. D.satpati,p.v.venkitakrishnan and a.biswas Doubt a study of glass and silicon carbidefiber reinforced ai{6061} hybrid composite for space application in slv f 21 37 (4) (2018), 5169-5165. (IOS-press) (SCIE) (I.F-1.637)

*** NATIONAL AWARDED & GOLD MEDAL

3. D.satpati and p.v.venkitakrishnan, s. Chatterjee doubt vhf radar measurement of momentum fluxes of gravity waves and tide over lower atmosphere over a tropical station in pslv fs

121 8(4) (2019), 101-121.(IGI Global) .(Scopus)

*** BEST SCHOLAR AWARDED & GOLD MEDAL

4. D.satpati and arghya biswas, Ch. 14. Doubt buckling and non-linear post buckling analysis of stiffened composite shells based on wavelet galerkin projection in gslv f 10, k.sivan and p.k. venkitakrisnan.

1-215 (2019), (IGI Global). doi:10. 978-91-7595-099-0

5. D.satpati and p.v.venkitakrisnan Doubt retrieval and budgeting of soil moisture and data monitoring from irs-p4{oceansat-1} mission data climate of isro., 5(1) (2019).

*** AWARDED GOLD MEDAL

6. D.satpati and sankha chatterjee Doubt study of short period gravity waves and associated momentum fluxes in the tropical middle atmosphere using mst radar and lider. 8 (4)(2020), 593-605. (Kyung MoonSa).

***INTERNATIONAL AWARDED

7. 5. D.satpati, p.v.venkitakrisnan AND sankhadeep agarwal Doubt remote sensing and budgeting of engine fuel device and data monitoring from irs-p5is{pslv c51-1} mission data climate of isro., 5(1) (2020).

*** AWARDED GOLD MEDAL

8. D.satpati,p.v.venkitakrishnan and a.biswas Doubt a study of sensing device and silicon carbidefiber reinforced ai{60645} hybrid composite for space application in pslv f 27 39ais (4) (2020), 5169-5165. (IOS-press) (SCIE) (I.F-1.637)

*** NATIONAL AWARDED & GOLD MEDAL